3D-modelling of conjugate heat and mass transfers: effects of storage conditions and species on wood high temperature treatment

Noura Oumarou*, Duygu Kocaefe, Yasar Kocaefe.

Université du Québec À Chicoutimi, Département des sciences appliquées, Chicoutimi (Québec), Canada

***Author to whom correspondence should be addressed**

☎ 001 418 545 50 11 # 5395

@ Noura_Oumarou@uqac.ca

✉ Université du Québec À Chicoutimi, Département des sciences appliquées, 555 Boulevard de l'Université, Chicoutimi (Québec), G7H 2B1 Canada

Abstract

Wood is definitely advantageous for industry because it is a renewable resource environment-friendly produced. However, the biological origin of wood requires some treatments to preserve and stabilise it. Heat treatment of wood at high temperature is one of the new techniques that reduce the hygroscopicity, improve dimensional stability, and increase resistance to biological degradation of wood material without the use of chemical products.

In this work, transient heat and mass transfers during heat treatment of wood at high temperature were numerically studied. The averaged energy Reynold Navier-Stokes equations and concentration equations for the fluid were coupled with the energy and mass conservation equations for the wood. The numerical conjugate problem considered also heat and mass exchange at the fluid-wood interface and was used to study the effects of specie-dependant (specific gravity) and storage-dependant (initial temperature and moisture content) parameters during the heat treatment. Both temperature and moisture content were affected by a low initial temperature during the first hours of the treatment, representing hypothetically a risk for wood quality. A high specific gravity or a high initial moisture content required supplemental heating time to reach the targeted final moisture content that potentially represent a supplemental energy and cost for industry.

Keywords: model, interface, wood, thermal treatment, species effect, storage effect

1. Introduction.

In the current battle against greenhouse gas emission, the wood material finds great importance in industrial applications because its production presents both low energy costs and benefits for carbon footprint. Wood is also a hygroscopic material with sophisticated multilayer cellular microstructure. Hence, it must be treated to build up dimensional stability and durability for industrial application. Heat treatment of wood has been considered as an effective method to modify wood without the use of any toxic chemicals.

Even though the effects of heat treatment for protection of wood were known for hundreds of years, industrial operations began quite recently. And only since last decades this issue has been scientifically studied and investigations on heat-treated wood at high temperature were subject of numerous publications [1-4]. Since 1990 different heat treatment processes for wood at high temperature were used in industries; including Finnish process (Thermo-Wood), Dutch process (Plato-Wood), French process (Bois-Rétifié, Bois-Perdure) and German process (Menz Holz or Oil-heat treatment) [5]. These technologies aim to implement a gradual rise in temperature of the wood in absence of oxygen. The high-temperature thermal treatments usually reach 150 - 260°C; that was an intermediate range of temperatures between the drying and the carbonization of the wood.

The heat treatment at high temperature of wood is known to improve its physical properties by reducing its hygroscopicity and increasing its dimensional stability [3, 6]. Also, Kamdem *et al.* [7] showed that the resistance of wood against decay by fungal attack was a friendly consequence of the heat treatment; and more broadly, thermal treatment of wood at high temperature is an effective method to improve its biological durability [8-12]. Chemical modifications of wood components occurring

during high temperature heat treatment are mainly responsible for these new properties [7, 13] and the decrease of hydroxyl groups, the increase of cellulose crystallinity and cross-linking occurring in lignin are both pointed out [14]. Furthermore, the targeted durability of the heat treated wood may vary significantly depending on the exposure conditions [15]. Thereby, heat-treated wood is usually not a suitable material for ground contact applications [16]. Beyond the targeted changes, heat treatment also causes adverse effects such as diminishing mechanical properties [17-20].

The high-temperature treatment is a complex process involving simultaneous heat, mass and momentum transfer phenomena. In consequence, effective models are helpful for process design, optimization, energy integration, and control [21-23]. Thus the problem can be numerically considered as a simultaneous heat and mass transfer through the porous medium [24, 25]. Furthermore, the theory of transport phenomena in porous materials has been itemized and reported in the literature [26-30]. Numerous models use a standard correlation to compute the heat and mass transfer at the interface of wood *in silico*. But *in situ*, high temperature treatment of wood is a transient conjugate problem in which the coefficients cannot be assumed as a constant throughout the wood surface. Thus, it is necessary to adapt models solving Navier–Stokes equations in the surroundings of the wood sample to get more information about the boundary conditions for the transport equations in the medium [31-33]. In some investigations, the classical Luikov model is used for the numerical formulation of the problem in wood [34-35] in order to analyse only the conjugate problem of heat and moisture transport. Kocaefe *et al.* [36] compared the different models for the thermal treatment of wood at high temperature (Diffusion, Luikov and Multiphase). The authors showed that the diffusion model was very useful for industrial

applications. Younsi and co-workers [37, 38] modelled heat treatment of wood by solving diffusion equations for heat and mass transfers in wood and turbulent Navier–Stokes equations in the fluid field. However, the mass and heat transfers in the wood were solved just using the mass and temperature continuity and their fluxes at the wood-fluid interface as boundary conditions [38, 39]. Now, the heat and mass transfers at the fluid-wood interface must be taken into account during the entire treatment in order to be close the real phenomena that are occurring during the heat process.

In this work, a three-dimensional model coupled the solved diffusion equations of heat and mass transfers for the wood sample with the turbulent averaged Navier–Stokes equations for the fluid flow field. The exchanges of heat and mass at fluid-wood interface were considered during the entire heating process by a subroutine which calculated the energy consumed by the wood and then injected it as a negative heat source in the gas energy computation. Our model was applied on some realistic industrial contexts. The final wood properties depend on both intrinsic such as the wood species and extrinsic parameters such as the wood storage conditions or the thermal process. Thus, industrial heat treatment of wood requires an efficient control of both the material and the process to obtain reproducibility and good quality. In this context, the model highlighted effects of one species-dependent parameter (specific gravity) as well as impact of some storage conditions resulting in several initial temperature and moisture content of wood.

2. Numerical method

High temperature treatment of wood is a complex problem where a conjugate simultaneous heat and mass transfer through porous medium occur. In this paper, the fluid flow field was coupled to the heat and mass transfers inside wood. The

numerical considerations involved solution of the hydrodynamic equations for the fluid followed by solving the equations of heat and mass transfers in wood. Thus, heat was transferred from heating gas to wood surface by convection and from surface to inside of the wood by conduction. Similarly, the moisture was transferred to the surface from the inside by diffusion and from the wood surface to the gas by convection.

2.1. Numerical assumptions

It was assumed that the flow field was turbulent, the fluid flow-porous system was three-dimensional, the temperature and moisture content were initially uniform inside the wood, the shrinkage and gravity effects were negligible, no degradation of the solid occurred during heat treatment and there was no heat generation inside the wood.

2.2. Balance governing equations for the fluid

The flow regime was assumed to be turbulent with respect to the average gas velocity measured in the furnace. The time-averaged Navier–Stokes equations and energy equation for turbulent flow with the Reynolds stresses, expressed *via* the eddy-viscosity concept, had been used as governing equations. The turbulence model used was the standard k–ε model for flows with high Reynolds number. The basis of this model was that the turbulent shear stresses were assumed to be related to strain rates *via* the eddy viscosity, which characterized the statistical properties of turbulent fluid. This eddy-viscosity property was obtained by solving two additional transport equations for the kinetic energy of turbulence k, and its dissipation rate ε.

The Standard k–ε Model [26, 35, and 40]:

Energy equation

$$\frac{\partial}{\partial t}\left(\rho_{\mathrm{f}} c_{\mathrm{pf}} T\right)+\frac{\partial}{\partial x}\left(\rho_{\mathrm{f}} u c_{\mathrm{pf}} T\right)+\frac{\partial}{\partial y}\left(\rho_{\mathrm{f}} v c_{\mathrm{pf}} T\right)+\frac{\partial}{\partial y}\left(\rho_{\mathrm{f}} w c_{\mathrm{pf}} T\right) = \frac{\partial}{\partial x}\left[\left(k_{\mathrm{eff}}\right)\frac{\partial T}{\partial x}\right]+\frac{\partial}{\partial y}\left[\left(k_{\mathrm{eff}}\right)\frac{\partial T}{\partial y}\right]+\frac{\partial}{\partial z}\left[\left(k_{\mathrm{eff}}\right)\frac{\partial T}{\partial z}\right] \quad (1)$$

Concentration equation

$$\frac{\partial}{\partial t}\left(\rho_{\mathrm{f}} C\right)+\frac{\partial}{\partial x}\left(\rho_{\mathrm{f}} u C\right)+\frac{\partial}{\partial y}\left(\rho_{\mathrm{f}} v C\right)+\frac{\partial}{\partial y}\left(\rho_{\mathrm{f}} w C\right) = \frac{\partial}{\partial x}\left[\left(D_{\mathrm{eff}}\right)\frac{\partial C}{\partial x}\right]+\frac{\partial}{\partial y}\left[\left(D_{\mathrm{eff}}\right)\frac{\partial C}{\partial y}\right]+\frac{\partial}{\partial z}\left[\left(D_{\mathrm{eff}}\right)\frac{\partial C}{\partial z}\right] \quad (2)$$

Continuity

$$\frac{\partial\left(\rho_{\mathrm{f}} U\right)}{\partial x}+\frac{\partial\left(\rho_{\mathrm{f}} U\right)}{\partial y}+\frac{\partial\left(\rho_{\mathrm{f}} U\right)}{\partial z}=0 \quad (3)$$

Momentum

- *X-momentum*

$$\frac{\partial}{\partial t}\left(\rho_{\mathrm{f}} u\right)+\frac{\partial}{\partial x}\left(\rho_{\mathrm{f}} u u\right)+\frac{\partial}{\partial y}\left(\rho_{\mathrm{f}} u v\right)+\frac{\partial}{\partial y}\left(\rho_{\mathrm{f}} u w\right) = -\frac{\partial p}{\partial x}+\frac{\partial}{\partial x}\left[\left(\mu_{\mathrm{eff}}\right)\frac{\partial u}{\partial x}\right]+\frac{\partial}{\partial y}\left[\left(\mu_{\mathrm{eff}}\right)\frac{\partial u}{\partial y}\right]+\frac{\partial}{\partial z}\left[\left(\mu_{\mathrm{eff}}\right)\frac{\partial u}{\partial z}\right] \quad (4)$$

- *Y-momentum*

$$\frac{\partial}{\partial t}\left(\rho_{\mathrm{f}} v\right)+\frac{\partial}{\partial x}\left(\rho_{\mathrm{f}} u v\right)+\frac{\partial}{\partial y}\left(\rho_{\mathrm{f}} v v\right)+\frac{\partial}{\partial y}\left(\rho_{\mathrm{f}} v w\right) = -\frac{\partial p}{\partial y}+\frac{\partial}{\partial x}\left[\left(\mu_{\mathrm{eff}}\right)\frac{\partial v}{\partial x}\right]+\frac{\partial}{\partial y}\left[\left(\mu_{\mathrm{eff}}\right)\frac{\partial v}{\partial y}\right]+\frac{\partial}{\partial z}\left[\left(\mu_{\mathrm{eff}}\right)\frac{\partial v}{\partial z}\right] \quad (5)$$

- *Z-momentum*

$$\frac{\partial}{\partial t}\left(\rho_{\mathrm{f}} w\right)+\frac{\partial}{\partial x}\left(\rho_{\mathrm{f}} u w\right)+\frac{\partial}{\partial y}\left(\rho_{\mathrm{f}} u w\right)+\frac{\partial}{\partial y}\left(\rho_{\mathrm{f}} w w\right) = -\frac{\partial p}{\partial z}+\frac{\partial}{\partial x}\left[\left(\mu_{\mathrm{eff}}\right)\frac{\partial w}{\partial x}\right]+\frac{\partial}{\partial y}\left[\left(\mu_{\mathrm{eff}}\right)\frac{\partial w}{\partial y}\right]+\frac{\partial}{\partial z}\left[\left(\mu_{\mathrm{eff}}\right)\frac{\partial w}{\partial z}\right] \quad (6)$$

K-Eddy kinetic energy

$$\frac{\partial}{\partial t}(\rho_f k)+\frac{\partial}{\partial x}(\rho_f uk)+\frac{\partial}{\partial y}(\rho_f vk)+\frac{\partial}{\partial y}(\rho_f wk)$$
$$=\frac{\partial}{\partial x}\left[\left(\mu+\frac{\mu_t}{\sigma_k}\right)\frac{\partial k}{\partial x}\right]+\frac{\partial}{\partial y}\left[\left(\mu+\frac{\mu_t}{\sigma_k}\right)\frac{\partial k}{\partial y}\right] \quad (7)$$
$$+\frac{\partial}{\partial z}\left[\left(\mu+\frac{\mu_t}{\sigma_k}\right)\frac{\partial k}{\partial z}\right]+p_k-\rho_f\varepsilon$$

ε-Rate of dissipation of turbulence energy

$$\frac{\partial}{\partial t}(\rho_f \varepsilon)+\frac{\partial}{\partial x}(\rho_f u\varepsilon)+\frac{\partial}{\partial y}(\rho_f v\varepsilon)+\frac{\partial}{\partial y}(\rho_f w\varepsilon)$$
$$=\frac{\partial}{\partial x}\left[\left(\mu+\frac{\mu_t}{\sigma_\varepsilon}\right)\frac{\partial \varepsilon}{\partial x}\right]+\frac{\partial}{\partial y}\left[\left(\mu+\frac{\mu_t}{\sigma_\varepsilon}\right)\frac{\partial \varepsilon}{\partial y}\right] \quad (8)$$
$$+\frac{\partial}{\partial z}\left[\left(\mu+\frac{\mu_t}{\sigma_\varepsilon}\right)\frac{\partial \varepsilon}{\partial z}\right]+\frac{\varepsilon}{k}(c_1 p_k-c_2\rho_f\varepsilon)$$

The production of turbulent kinetic energy due to the viscous forces was modeled using the following expression:

$$p_k=\mu_t\left[2\left(\left(\frac{\partial u}{\partial x}\right)^2+\left(\frac{\partial v}{\partial x}\right)^2+\left(\frac{\partial w}{\partial x}\right)^2\right)+\left(\frac{\partial u}{\partial x}+\frac{\partial v}{\partial x}+\frac{\partial w}{\partial x}\right)^2\right] \quad (9)$$

$$\mu_{\text{eff}}=\mu+\mu_t,\ k_{\text{eff}}=k_f+\mu_t c_{pf}/\sigma_T,\ D_{\text{eff}}=D+\mu_t/\sigma_C,\ \mu_t=C_\mu\rho_f k^2/\varepsilon$$

The values of the model constants for all the models considered are σ_k=1.0, σ_ε=1.4, σ_T=1.0, σ_C=1.0, C_1=1.44, C_2=1.92, Cμ=0.09.

The model of turbulences presented above was valid only in the fully turbulent region. In regions close to the wall, viscous effects predominated over turbulence effects, due to the small local Reynolds number of turbulence. To account for these regions for computing turbulent flows, the classical wall function method [26, 35, and 40] was followed. The wall functions were used to bridge the near-solid-wall region in the case of the standard k–ε model. The integration of k and ε equations from fully turbulent region to the wall resulted in the following equation for the wall shear stress:

$$\tau_w = \frac{\rho_f C_\mu^{1/4} k^{1/2}}{\ln\left(y^+\right)} U \tag{10}$$

Where U was the average velocity component parallel to the wall (u for the wall in x direction, v for the wall in y direction and w for the wall in z direction). Similarly, the following expression was obtained for the ε near the wall region:

$$\varepsilon = \frac{C_\mu^{3/4} k^{3/2}}{C_k y} \ln\left(C_k y^+\right) \tag{11}$$

2.3. Balance governing equations for solid wood

During heat treatment, a combination of transfer mechanisms occurred simultaneously in a porous material like wood due to its microscopic capillaries and pores. Two modes of diffusion processes occurred in the wood sample [41] during heat treatment at high temperature. With respect to above considerations, the three-dimensional equations describing heat and mass transfers in wood during heat treatment at high temperature were given by [41, 42]:

Heat transfer equation

$$\rho_m \frac{\partial h_m}{\partial t} = \frac{\partial}{\partial x}\left(k_{qx} \frac{\partial T}{\partial x}\right) + \frac{\partial}{\partial y}\left(k_{qy} \frac{\partial T}{\partial y}\right) + \frac{\partial}{\partial z}\left(k_{qz} \frac{\partial T}{\partial z}\right) \tag{12}$$

Moisture transfer equation

$$\frac{\partial M}{\partial t} = \frac{\partial}{\partial x}\left(D_x \frac{\partial M}{\partial x}\right) + \frac{\partial}{\partial y}\left(D_y \frac{\partial M}{\partial y}\right) + \frac{\partial}{\partial z}\left(D_z \frac{\partial M}{\partial z}\right) \tag{13}$$

2.4. Initial and Boundary conditions

The wood material undergoing heat treatment was supposed to have initially uniform temperature and moisture content throughout. Thus the initial conditions were expressed as:

Temperature uniformity:

$$T\left(x,y,z,0\right)=T_0 \tag{14}$$

Moisture content uniformity:

$$M\left(x,y,z,0\right)=M_0 \tag{15}$$

In all the steps, the boundary conditions were expressed in terms of the continuity of state variables and their respective fluxes at the interface [43]. The equations were represented as follows:

Temperature Continuity :

$$T_f = T_S \tag{16}$$

Concentration Continuity :

$$C_f = C\left(T,M\right)_S \tag{17}$$

Energy Transfer at the wood-fluid interface :

$$\left[k_q \frac{\partial T}{\partial n}\right] = \Delta H_{lV} D \frac{\partial C_f}{\partial n} + k_f \frac{\partial T}{\partial n} \tag{18}$$

Mass Transfer at the wood-fluid interface :

$$\left[\rho_d D_S \frac{\partial M}{\partial n}\right] = D \frac{\partial C_f}{\partial n} \tag{19}$$

The boundary conditions (inflow and outflow) for the flow fields were considered as:

In flow : $u=0, v=U_g, w=0, T=T_g, C=C_g, k=k_{in}, \varepsilon=\varepsilon_{in}$

Outflow : $P=0, \partial T/\partial y=0, \partial C/\partial y=0, \partial k/\partial y=0, \partial \varepsilon/\partial y=0.$

2.5 Thermo physical properties of Wood

The realistic modelling of heat transfer and mass transfer in wood is a complex phenomenon that takes into account not only the heat conduction, the moisture diffusion in wood, the chemical decomposition of wood, but also variations in the

specific gravity, density, moisture content, thermal conductivity and heat capacity. The present numerical study focused on two wood species: Aspen (*Populus tremuloides*) which has a specific gravity of 0.4 and Ash (*Fraxinus americana*) which has 0.63 as specific gravity [44]. The thermodynamic and transport properties of gas-water system and the physical properties of the two wood species used in the simulation are summarised in Table 1. The density (ρ), specific gravity (G_m), thermal conductivity (k_{qx}, k_{qy}, k_{qz}) and heat capacity (C_P) of wood were calculated using expressions proposed by Simpson and Tenwolde [44] and Siau [41].

$$\rho = 1000 G_m \left(1 + M/100\right) \tag{20}$$

The heat capacity of wood depends on the temperature and moisture content in the wood, but does not depend on the density of wood species [44]. The heat capacity of dry wood C_{P0} (kJ/kg /K) was approximately related to temperature T by:

$$C_{P0} = 0.1031 + 0.003867T \tag{21}$$

The heat capacity of the wood containing water (green wood) is higher than that of dry wood. Below the point of fibre saturation, the heat capacity was the sum of heat capacity of dry wood, that of water and factor B_C which involved the additional energy in the wood.

$$C_P = \left(C_{P0} + 0.01 M C_{PW}\right) / \left(1 + 0.01M\right) + B_C \tag{22}$$

where M was the moisture content (%). The heat capacity of water was about 4.19 kJ/kg.K. The adjustment factor B_C was deducted from the following expression:

$$B_C = M\left(\text{-}0.06191 + 2.36\ 10^{\text{-}4}\ T + \text{-}1.33\ 10^{\text{-}4}\ M\right) \tag{23}$$

The thermal conductivity is a measure of the heat flow rate through unit area of a material subjected to a temperature gradient. The thermal conductivity of wood is

affected by numerous factors such as density, moisture content, grain direction, structural irregularities and temperature. Thermal conductivity has approximately the same value in the radial and tangential directions while it is about two times greater along the grain [45]. For moisture levels below the saturation point of the fibre, the thermal conductivity in directions orthogonal to the grain (radial and tangential) was given by a linear equation:

$$k_{qx} = k_{qz} = A_1 + G_m\left(A_2 + A_3 M\right), \qquad \left(k_{qy} = 2k_{qx} = 2k_{qz}\right) \tag{24}$$

Where A_1, A_2 and A_3 were constants given by: $A_1 = 0.01864$, $A_2 = 0.1941$ and $A_3 = 0.004064$.

The latent heat of vaporization was correlated with temperature by a polynomial function [45]:

$$\Delta H_{lV} = 2.792.10^6 - 160(T) - 3.43(T)^2 \tag{25}$$

3. Numerical material

The mathematical equations of the coupling system were resolved in two parts. The solutions of hydrodynamic equations for the flow of gas in the furnace were obtained using the commercial software ANSYS CFX-10 [46]. The results were used to assess, for each time step, the temperature and mass gradients at particularly wood-fluid interface, which were then used as boundary conditions for heat and mass transfers of wood. A subroutine based on the finite difference method was developed using FORTRAN to solve the equations of heat and mass transfers. The solution of the matrix was obtained using the method of Gauss-Seidel iterative at each time step. Exchanges of heat and mass at wood-fluid interface were considered. The model of coupling thermofluid described above was optimized for sensitivity to the number of

iterations, the time steps and the refining mesh. All calculations were made with optimized refined meshes.

4. Experimental

The experiments were performed using a prototype furnace at the University of Québec at Chicoutimi (Canada). The wood samples were boards (0.05m x 0.20m x 1.24m). The furnace simultaneously treated from 60 to 80 wood boards. The wood species tested were chosen to explore a large G_m range; from G_m = 0.4 (*i.e.* Aspen, *Populus tremuloides*) to G_m = 0.71 (*i.e.* birch, *Betula papyrifera*). The initial moisture content of wood samples (M_0) was measured before each experiment using a wood moisture meter Delmhorst RDM-2S (0.1% accuracy). The maximum temperature was 210°C (483 K) and a gently gradient was applied (which did not exceed 12 ± 2 °C per hour) to reduce mechanical degradation of wood and maintain a high quality. The temperature was estimated every minute by the mean of the readings from several positions within the wood boards. T-type thermocouples were connected to the data acquisition system Keithley KE 2700-Omnitronix TC4000 (3.8% accuracy). The experimental values were compared to the modelled ones using JMP 11 (SAS© Institute Inc., Cary, NC, USA).

5. Results and discussion

5.1. Modelled *vs.* experimental temperatures

The modelled wood temperatures were close the experimental ones into the 0.4-0.71 specific gravity range (figure 1). Their relationship was linear (y = 0.995 x; r^2 = 0.997) and values were within the 95% confidence interval. The two species explored in this study were into this validated range; presenting specific gravity G_m = 0.40 and

G_m = 0.63. These values corresponded to specific gravities of dry Aspen quaking and white Ash respectively [44].

5.2. Effect of the specific gravity

The impact of heat treatment on final wood properties is usually species-dependent [47]. The model was used to highlight the role of the specific gravity (G_m) in the differences observed between species. The evolution of temperature and moisture content predicted by the model along the 16h-treatment were shown in the figure 2, for two species for which G_m = 0.4 and 0.63 (Aspen and Ash respectively).

At the surface or at the center of wood, the higher was the value of specific gravity the lower was the wood temperature during the heat treatment (figure 2a). Indeed, high specific gravity value corresponded to a dense wood [41]; which contained a lot of water and a few air in its holes. Thus a high specific gravity condition resulted in the high value of moisture content observed (figure 2 b); and, in consequence, energy required to heat high specific gravity wood would be higher than energy needed for low specific gravity wood. As temperature decreased when the specific gravity increase (figure 2a), the wood also presented a low diffusivity when the specific gravity was high (figure 3). Consequently the transfer of heat from wood surface (exposed to heating fluid flow) to the center was slow for the great specific gravity. On the other side, the moisture content was removed at a faster rate if the value of specific gravity was low (figure 2b). At the wood center, the moisture content started to get removed after about six hours for G_m = 0.4 and 10 hours for G_m = 0.63. It may be noted that for both of the wood species, the moisture removal was more important near the surface than at center. Due to the low thermal diffusion (figure 3), the temperature gradient vanished at the middle of the wood for the highest value of specific gravity. The higher was the specific gravity, the less was heat diffusion within

wood sample and the more difficult was to remove the moisture content from wood center. Hence, in this case, the gradient of moisture content remained quite high even at the end of heat treatment (figure 2b). These results were in accordance with some previous experiments demonstrating that the chemical structure (decrease in number of hydroxyl groups) of birch (high G_m) was more affected by heat treatment at high temperature than the one of Aspen (low G_m) [47].

5.3. Importance of the initial temperature and moisture content

In order to understand and optimise the heat treatment process, two external parameters were studied: initial temperature and initial moisture content of wood. These parameters are usually a result of the wood storage conditions. Two values of temperature (T_0 = 0°C and 25°C) and moisture content (M_0 = 12% and 30%) were tested as the initials conditions (table 1). The other parameters like wood properties, fluid flow field, the way that wood was heated, final temperature reached, were kept the same for all the four investigations.

5.3.1. Initial temperature

The figure 4 illustrated the prediction for the temperature and moisture content changes within the wood sample, for T_0 = 0°C or T_0 = 25°C. The temperature was higher at the sample surface exposed to heating fluid flow than that at center for both initial temperature conditions (figure 4a). The temperature distributions differed early depending whether T_0 = 0°C or T_0 = 25°C. When the heating time increases, this difference diminished gradually and vanished for high value of heating time. In order to clearly identify this early impact on heat propagation inside the wood, the temperature variation along x direction was plotted for different heating times (figure 5). The change of temperature gradient between the material surface and its center was more important when initial temperature is low, particularly at the start of heat

treatment. This high temperature gradient reduced gradually with time and became similar to that for T_0 = 25°C after about six hours (figure 5).

The moisture content removal was less affected by the initial temperature condition (figure 4b). No impact was observed at wood center. However, it should be noted that a little effect was observed at the surface but disappeared when the moisture at the wood center started to get removed (about seven hours). Hence, more attention must be given in the range where temperature rise and moisture evaporation were affected by initial temperature condition, to avoid any unwanted swelling or shrinkage of wood material.

5.3.2. Initial moisture content

The final properties of heat-treated wood always depend on its moisture content. So, with respect to its initial moisture content, the behaviour of wood undergoing thermal treatment at high temperature needed to be understood and clarified in a better way. In this context, wood samples with two initial moisture content (M_0 = 12% and 30%) were investigated. The results were illustrated in figures 6 and 7. The temperature rise with increase in time was distinctly affected by a change of initial moisture content in the wood material (figure 6a). This change occurred not only at the surface but also at the inside of the wood broad. For a fixed specific gravity, the wood porosity decreased when its moisture content increases and consequently its density became high [44]. Hence, the more was the initial moisture content in wood; the less was the temperature at each point of sample (figure 6a and 7) during the thermal treatment. The changes in ratio of moisture content to initial moisture (M/M_0) along a 16h-treatment was plotted in figure 6b to quantify the moisture losses during high temperature treatment. The moisture content in the wood was removed quickly when the initial value is low. For example, close to the surface, half of the initial moisture

content in the wood got removed after five hours of heating for M_0 = 12% against ten hours when M_0 = 30% (figure 6b). At the end of heat treatment (16 hours), 68% of moisture content was evacuated from the wood center in the case where M_0 = 12% against only 23% when M_0 = 30% (figure 6b). In consequence, high initial moisture treatment needed a long-time heating process to reach a good wood quality that would increase energy supplies and costs for industry.

6. Conclusions

The model predicted the impact of specific gravity, initial conditions of temperature and moisture content on thermal treatment of wood sample at high temperature. The quality of the final heat treated wood depends not only on its species, but also on the external process conditions. Supplemental heating time is required to remove the desired amount of moisture when the wood material has a high specific gravity or a high initial moisture content. That may increase energy supply and costs during the heating. When initial temperature is low, operators may pay attention to the first hours of heat process to avoid any unwanted swelling or shrinkage of wood material at the surface. The model was useful for the wood behaviour prediction under high thermal treatment.

Nomenclature

Symbols

C	Concentration ($kg.\ m^{-3}$)
C_P	Heat capacity ($J.\ kg^{-1}.\ K^{-1}$)
D	Diffusion coefficient of water vapour in the fluid ($m^2.\ s^{-1}$)
D_s	Diffusion coefficient in the wood material ($m^2.\ s^{-1}$)

G_m	Specific gravity
k	Turbulent kinetic energy ($m^2. s^{-2}$)
h_q	Convective heat transfer coefficient ($W. m^{-2}. K^{-1}$)
k_f	Thermal conductivity of fluid ($W. m^{-1}. K^{-1}$)
k_q	Thermal conductivity of wood ($W. m^{-1}. K^{-1}$)
M	Moisture content, kg H_2O $(kg\ solid)^{-1}$
P	Pressure (Pa)
P_k	Shear production of turbulent kinetic energy ($m^2. s^{-3}$)
T	Temperature (K)
(x,y,z)	Spatial coordinates (m, m, m)
(v, u, w)	Average velocity ($m. s^{-1}$)

Greek letters

ρ	Mass density ($kg. m^{-3}$)
μ	Dynamic viscosity ($kg. m^{-1}. s^{-1}$)
ε	Viscous dissipation in turbulent flows
$\sigma_{k,\varepsilon,T,C}$	Turbulent Prandtl numbers of k, ε, T and C
τ_W	Wall shear stress ($N. m^{-2}$)
ΔH_{lv}	Latent heat of vapourisation ($J. kg^{-1}$)

Subscripts

0	Initial
d	Dry porous solid
eff	Effective value
bt	Bound
f	Fluid
Y^*	Dimensionless distance from wall in turbulent flow

Acknowledgments

The authors gratefully thank Le Fonds Québécois de la Recherche sur la Nature et les Technologies (FQRNT), University of Quebec at Chicoutimi (UQAC), Foundation of UQAC (FUQAC), Développement Économique Canada (DEC), Ministère du Développement Économique, de l'Innovation et de l'Exportation (MDEIE), Conférence Régionale des Élus du Saguenay-Lac-St-Jean (CRÉ) for their financial support. The Alberta Research Council, Cégep de Saint-Félicien, Forintek, PCI Ind., Ohlin Thermotech, Kisis Technology, and Industries ISA are also acknowledged for their contribution. We also appreciated the technical help in the CFX use from Dr. RamdaneYounsi and the comments on the manuscript from Dr. Angélique Lazartigues.

References

[1] A. J. Stamm, Heat-stabilized wood, Industrial and Engineering Chemistry 38 (6) (1946) 630-634.

[2] J. Bourgois and R. Guyonnet, Characterization and Analysis of Torrefied Wood, Wood Science & Technology 22 (2) (1988) 143-155.

[3] P. Kamdem, A. Pizzi, M. C. Triboulot, Heat treated timber: potentially toxic byproducts presence and extent of wood cell wall degradation, Holz als Roh-und Werkstoff 58 (4) (2000) 253-257.

[4] Y. Xie, Y. Liu, Y. Sun, Heat-treated wood and its development in Europe, Journal of Forestry Research 13 (3) (2002) 224 -230.

[5] Steves 2007a B. Esteves, I. Domingos and H. Pereira, Improvement of technological quality of eucalypt wood by heat treatment in air at 170-200ºC, Forest Products Journal 57 (1,2), (2007a) 47-52

[6] A. J. Santos, Mechanical behavior of eucalyptus wood modified by heat, Wood Science and Technology 34 (1) (2000) 39-43.

[7] D. Kamdem, A. Pizzi, A. Jermannaud, Durability of heat-treated wood, Holz als Roh und Werkstoff 60 (1) (2002) 1-6.

[8] I. Momohara, W. Ohmura, H. Kato, Y. Kubojima, Effect of high-temperature treatment on Wood durability against the brown-rot fungus, Fomitopsis palustris, and the Termite Coptotermes formosanus, 8th International IUFRO Wood Drying Conference, 2003.

[9] M. Hakkou, M. Pétrissans, P. Gerardin, A. Zoulalian, Investigations of the reasons for fungal durability of heat-treated beech wood, Polymer Degradation and Stability 91 (2) (2006) 393–397.

[10] J. L. Shi, D. Kocaefe, T. Amburgey, J. Zhang, A comparative study on brown-rot fungus decay and subterranean termite resistance of thermally-modified and ACQ-C-treated wood, Holzals Roh-und Werkstoff 65 (5) (2007) 353-358.

[11] J. L. Shi, D. Kocaefe, J. Zhang, Mechanical behaviour of Québec wood species heat-treated using ThermoWood process, Holz als Roh- und Werkstoff 65 (4) (2007) 255–259.

[12] S. Poncsak, S. Q. Shi, D. Kocaefe, G. Miller, Impact of the thermal treatment on the adhesion between different wood species and adhesives, Journal of Adhesion Science and Technology 21 (8) (2007) 745–754.

[13] S. Mouras, P. Girard, P. Rousset, P. Permadi, D. Dirol and G. Labat, Physical properties of non durable woods with a low temperature pyrolysis treatment - Proprietes physiques de bois peu durables soumis à un traitement de pyrolyse ménagée. Annals of Forest Science 59 (3) (2002) 317-326.

[14] B.M. Esteves, and H.M. Pereira, Wood modification by heat treatment: A review, BioResources 4 (1) (2009), 370-404.

[15] M. Kutnik, E. Suttie and C. Brischke, European standards on durability and performance of wood and wood-based products based products trends and challenges, Wood material science and engineering (2014) *In press*, DOI: http://dx.doi.org/10.1080/17480272.2014.894574

[16] S. Jamsa, and P. Viitaniemi, Heat treatment of wood. Better durability without chemicals. In: Proceedings of COST E22 environmental optimisation of wood protection, Antibes, France (2001) 21-26.

[17] B. M. Esteves, I. J. Domingos and H. M. Pereira, Pine wood modification by heat treatment in air, Biroresources 3 (1) (2008a) 142-154.

[18] B. Esteves, A. V. Marques, I. J. Domingos and H. M. Pereira, Influence of steam heating on the properties of pine (Pinus pinaster) and eucalypt (Eucalyptus globulus) wood, Wood Science Technology 41 (2007b) (3) 193-207.

[19] J. L. Shi, D. Kocaefe and J. Zhang, Mechanical behaviour of Quebec wood species heat-treated using thermo wood process, Holz Roh Werkst 65 (4) (2007) 255-259.

[20] S. Korkut, The effects of heat treatment on some technological properties in Uludag fir (Abies bornmullerinana Mattf) wood, Build Environ 43 (2008a) 422-428.

[21] C. Fhyr, A. Rasmuson, Some aspects of the modelling of wood chips drying in superheated steam, International Journal of Heat and Mass Transfer 40 (12) (1997) 2825–2842.

[22] A. Johanson, C. Fhyr, A. Rasmuson, High temperature convective drying of chips with air and superheated steam, International Journal of Heat and Mass Transfer 40 (12) (1997) 2843-2858.

[23] S. Pang, Relative importance of vapour diffusion and convective flow in modelling of softwood drying, Drying Technology 16 (1,2) (1998) 271–281.

[24] R. Younsi, S. Poncsak, D. Kocaefe, Experimental and Numerical Investigation of Heat and Mass Transfer during high-temperature Thermal Treatment of Wood, Drying Technology 28 (10) (2010) 1148-1156.

[25] R. Younsi, D. Kocaefe, S. Poncsak, Y. Kocaefe, Computational modeling of heat and mass transfer during the high-temperature heat treatment of wood, Applied Thermal Engineering 27 (8,9) (2007) 1424-1431.

[26] A. V. Luikov, Systems of differential Equations of Heat and Mass Transfer in Capillary-porous Bodies, International Journal of Heat Transfer 18 (1) (1975) 1-14

[27] A. V. Luikov, Heat and Mass Transfer, Mir, Moscow (1980).

[28] S. Whitaker, Simultaneous Heat, Mass and Momentum Transfer in Porous Media: A Theory of Drying, Advances in Heat Transfer 13 (1977) 119-203.

[29] S.A. Bories, Fundamentals of drying of capillary-porous bodies, in: S. Kakac, B. Kilkis, F.A. Kulacki, F. Arinc Dordrecht (Eds.), Convective heat and mass transfer in porous media, Kluwer Academic Publishers, The Netherlands, 1991.

[30] M. Ahiua, L. Yi, Numerical heat transfer coupled with multidimensional liquid moisture diffusion in porous textiles with a measurable parameterized model, Numerical Heat Transfer, Part A: Application 56 (3) (2009) 246–268.

[31] R. Younsi, D. Kocaefe, S. Poncsak, T. Junjun, Numerical and experimental validation of the transient heat and mass transfer during heat treatment of pine wood, International Journal of Modelling and Simulation 28 (2) (2008) 117–123.

[32] R. Younsi, D. Kocaefe, S. Poncsak, Y. Kocaefe, L. Gastonguay, CFD modeling and experimental validation of heat and mass transfer in wood poles subjected to high temperatures: a conjugate approach, Journal of Heat and Mass Transfer 44 (12) (2008) 1497–1509.

[33] R. Younsi, D. Kocaefe, S. Poncsak, Y. Kocaefe, L. Gastonguay, A high-temperature thermal treatment of wood using a multiscale computational model: Application to wood poles, Bioresource Technology 101 (12) (2010) 4630–4638.

[34] R. Younsi, D. Kocaefe, Y. Kocaefe, Three-dimensional simulation of heat and 364 moisture transfer in wood, Applied Thermal Engineering 26 (11,12) (2006) 1274–1285.

[35] R. Younsi, D. Kocaefe, S. Poncsak, Y. Kocaefe, Thermal modeling of the high 367 temperature treatment of wood based on Luikov's approach, International Journal of Energy Research 30 (9) (2006) 699–711.

[36] D. Kocaefe, R. Younsi, S. Poncsak, Y. Kocaefe, Comparison of different models for the high-temperature heat-treatment of wood, International Journal of thermal Science 46 (7) (2007) 707-716

[37] R. Younsi, D. Kocaefe, S. Poncsak, Y. Kocaefe, A Diffusion-based Model for Transient High Temperature Treatment of wood, Journal of Building Physics 30 (2) (2006) 113-135.

[38] R. Younsi, D. Kocaefe, S. Poncsak, Y. Kocaefe, Computational and experimental analysis of high temperature thermal treatment of wood based on thermoWood technology, International Communications in Heat and Mass Transfer 37 (1) (2010) 21-28.

[39] D. Kocaefe, Y. Kocaefe, R. Younsi, N. Oumarou and S. Thierry Lekounougou, Mathematical modeling of the high temperature treatment of birch in a prototype furnace, Advances in Mechanical Engineering, 2013 (2013), in press DOI: http://dx.doi.org/10.1155/2013/194610.

[40] P. Majumdar, P. Deb, Computational analysis of turbulent fluid flow and heat transfer over an array of heated modules using turbulence models, Numerical Heat Transfer, Part A: Applications: An International Journal of Computation and Methodology 43 (7) (2003) 669-692.

[41] J. F. Siau, Transport processes in wood. Springer, New York (1984).

[42] M. d. Raisul Islam, J. C. Ho, and A. S. Mujumdar, Simulation of Liquid Diffusion-Controlled Drying of Shrinking Thin Slabs Subjected to Multiple Heat Sources, Drying technology 21 (3) (2003) 413–438.

[43] K. Murugesan, H. N. Suresh, K. N. Seetharamu, P. A. A. Narayana, T. Sundararajan, A theorical model of brick drying as a conjugate problem. International Journal of Heat and Mass Transfer 44 (21) (2001) 4075-4086.

[44] W. Simpson, A. Tenwold, Physical properties and moisture relations of wood ; Wood handbook, USDA Forest service, Forest product laboratory, Madison, WI, USA, vol.3 (1999) pp. 1-23.

[45] M. A. Stanish, G. S. Schajer, F. Kayihan, A mathematical model of drying for hygroscopic porous media, American Institute of Chemical Engineers journal 32 (8) (1986) 1301–1311.

[46] CFX-10 User Manual, ANSYS CFX, 2005.

[47] D. Kocaefe, B. Chaudhry, S. Poncsak and Y. Boluk, Effect of thermal treatment on the chemical composition properties of Birch and Aspen, BioRessources 3 (2) (2008) 517-537.

Table 1. Wood properties and initial conditions [41]

Parameter range values	*Parameter expression*
	– –

Figure 1. Validation of the model by experiment for species which had specific capacity (G_m) ranging from 0.4 to 0.71 (y=0.995x, r^2 = 0.997; confidence interval 95%).

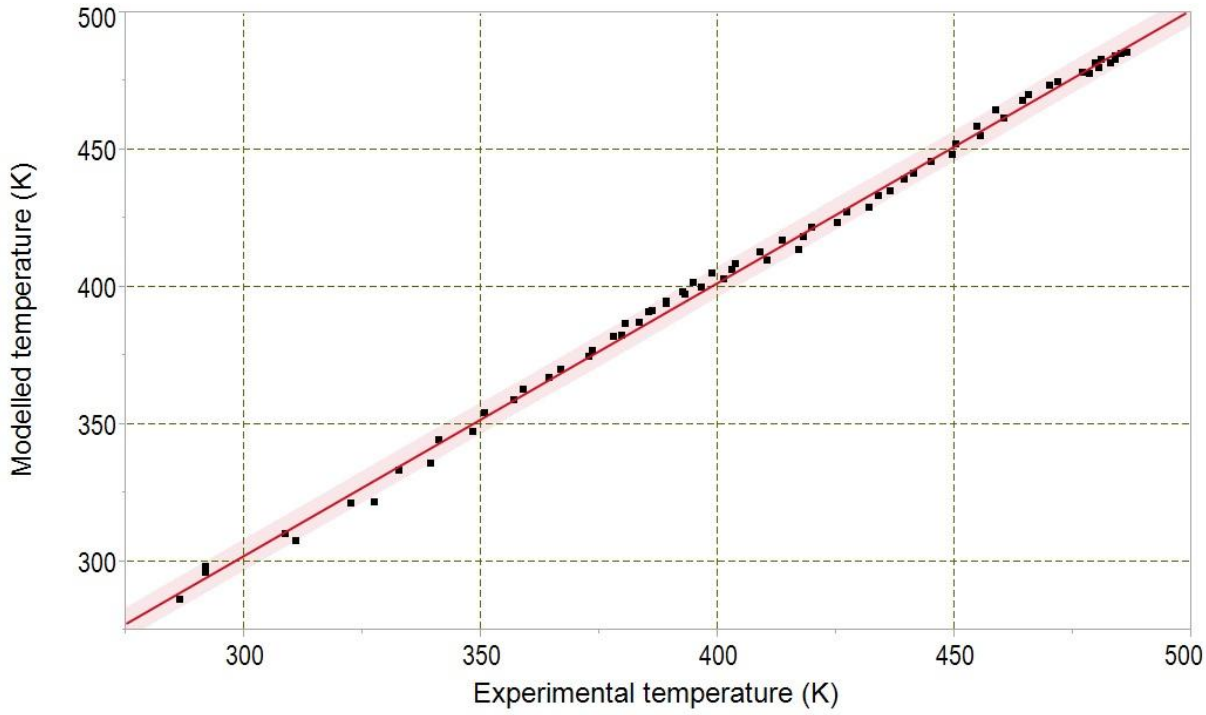

.

Figure 2. Predicted (a) temperature and (b) moisture content at the center and the surface of a wood broad during a 16h-heating, for aspen (G_m = 0.40) and ash (G_m = 0.63).

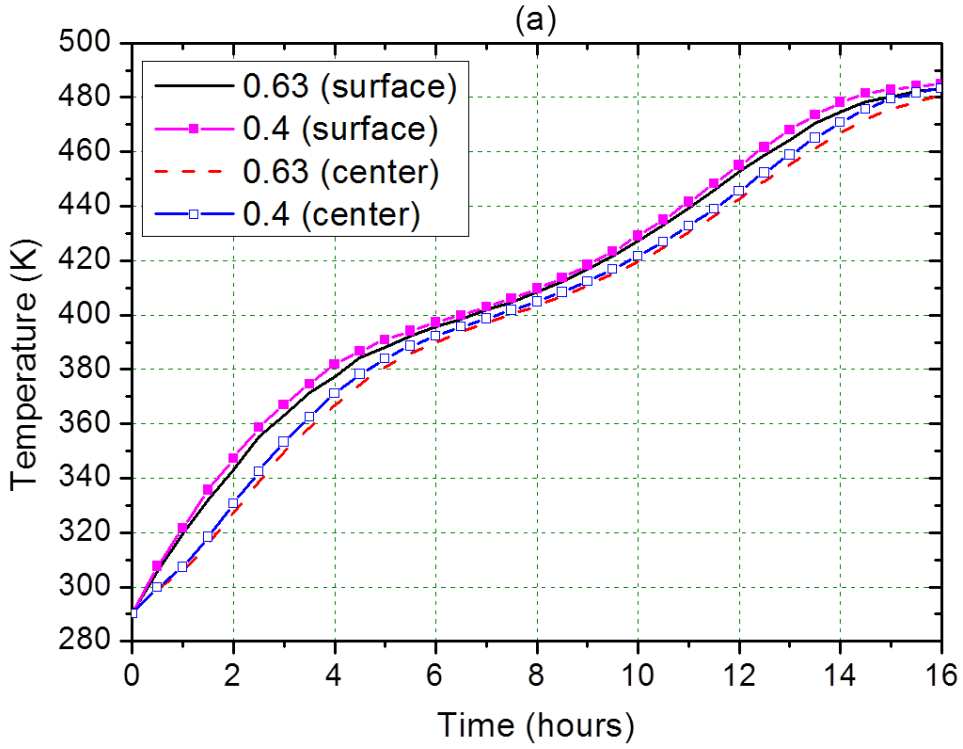

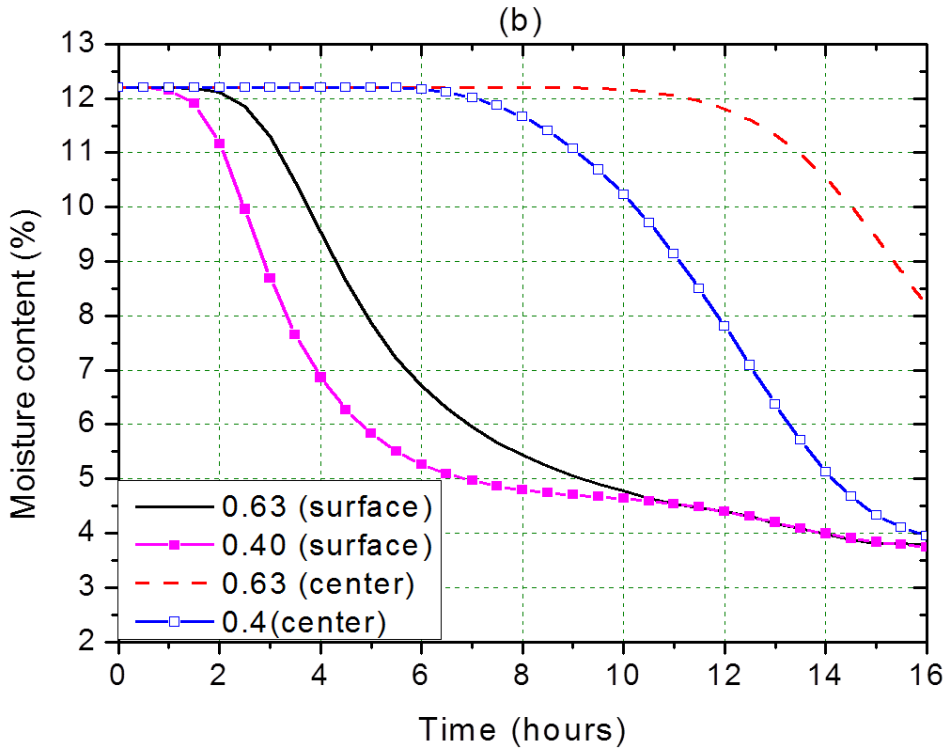

Figure 3. Predicted thermal diffusivity during a 16h-heating for aspen (G_m = 0.40) and ash (G_m = 0.63).

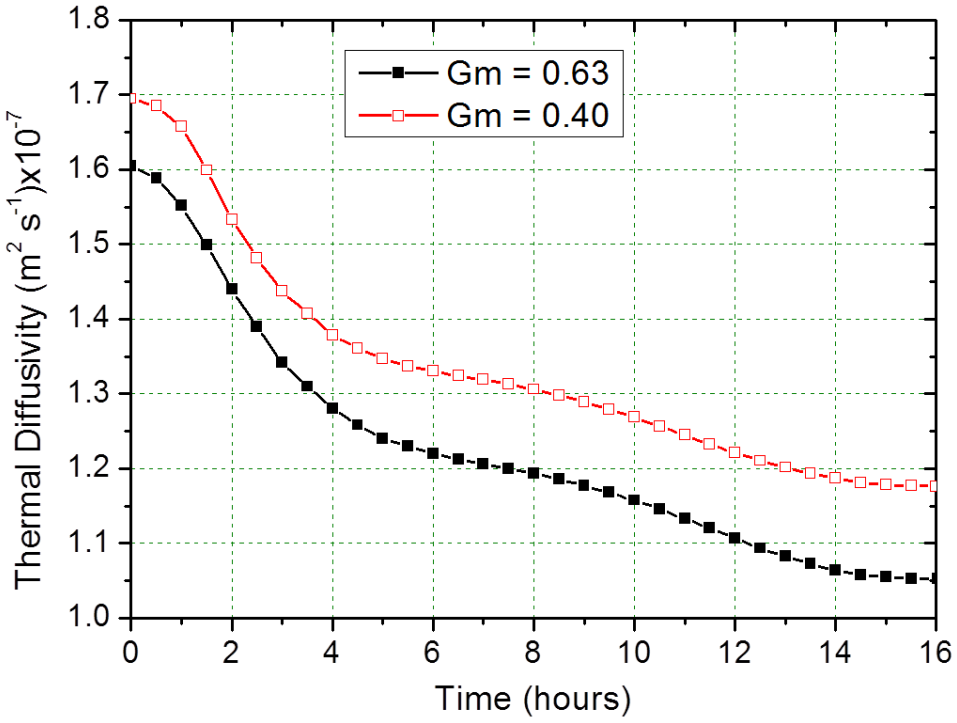

Figure 4. Predicted (a) temperature and (b) moisture content during a 16h-heating for two initials temperatures conditions (T_0 = 0°C and T_0 = 25°C, G_m = 0.4).

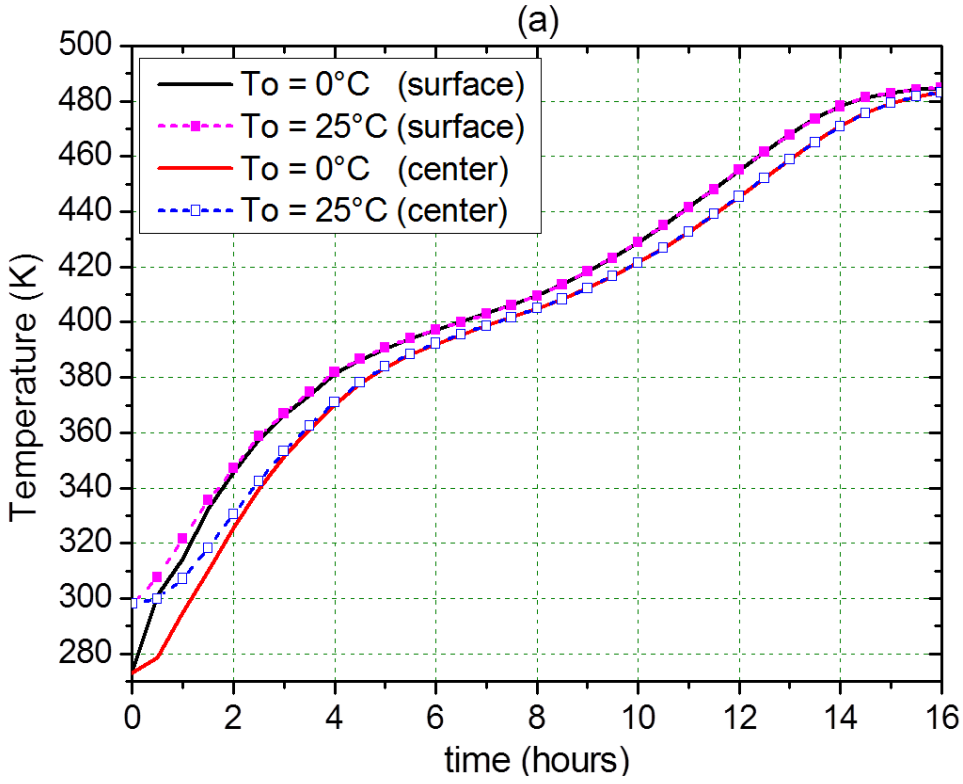

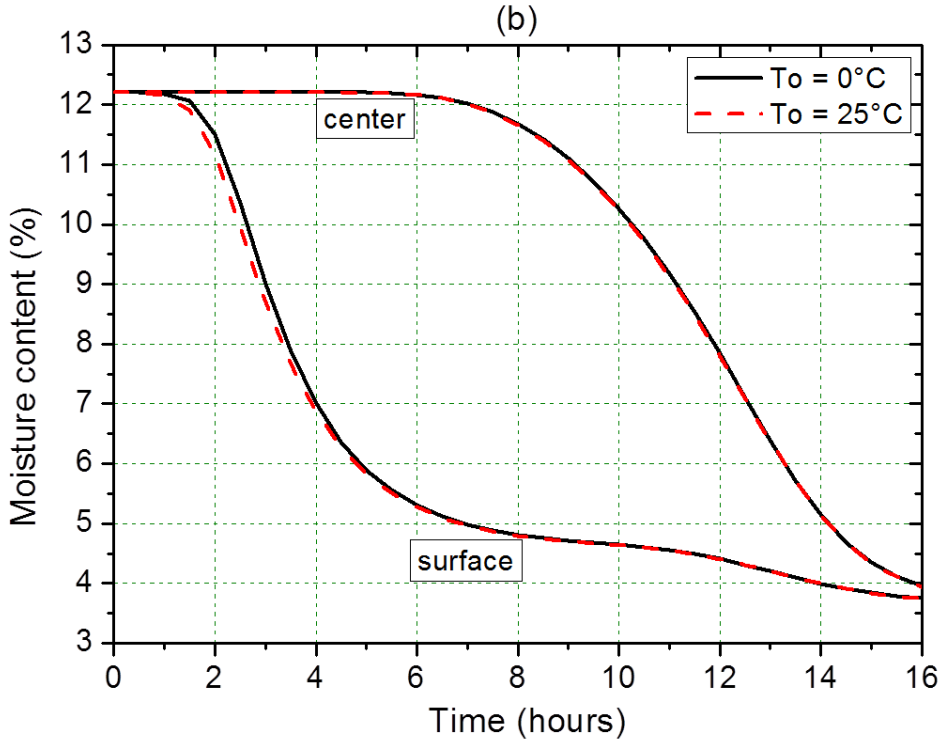

Figure 5. Temperature distribution along the x direction for two initials temperatures conditions (T_0 = 0°C and T_0 = 25°C, G_m = 0.4).

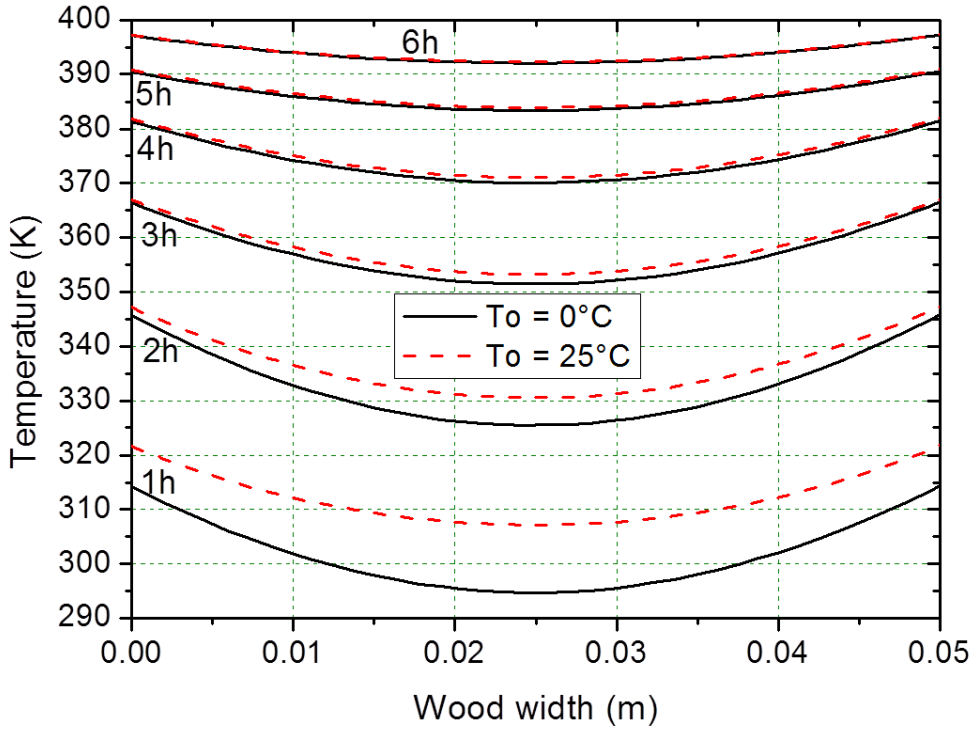

Figure 6. Predicted (a) temperature and (b) moisture contents ratio (M/M_0) during a 16h-heating for two initials moistures conditions (M_0 = 12% and M_0 = 30%, , G_m = 0.4).

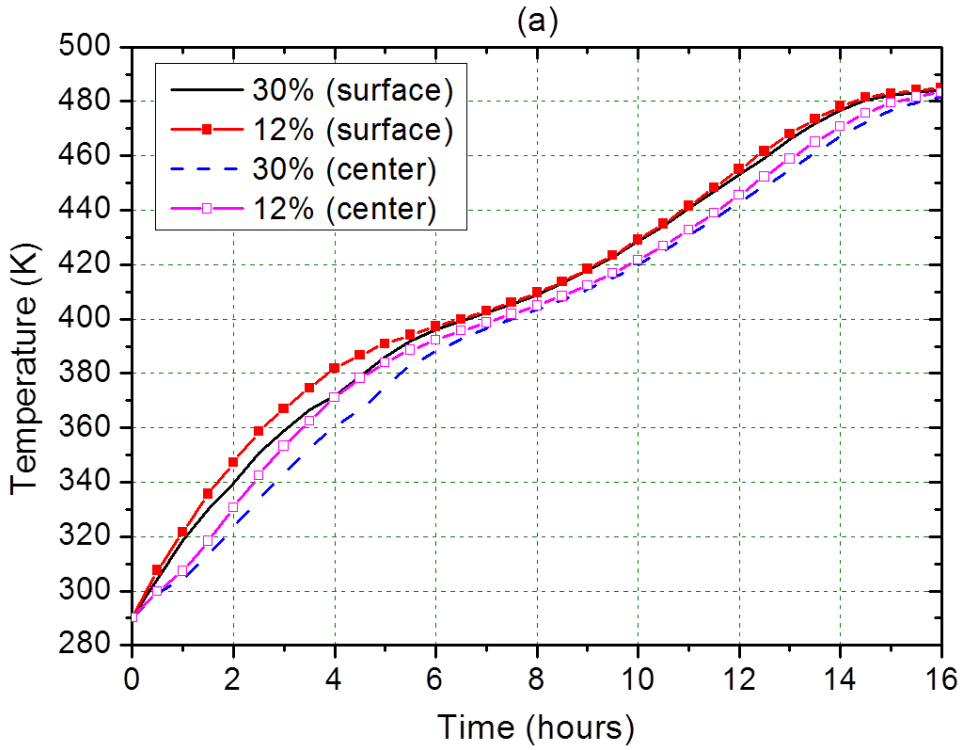

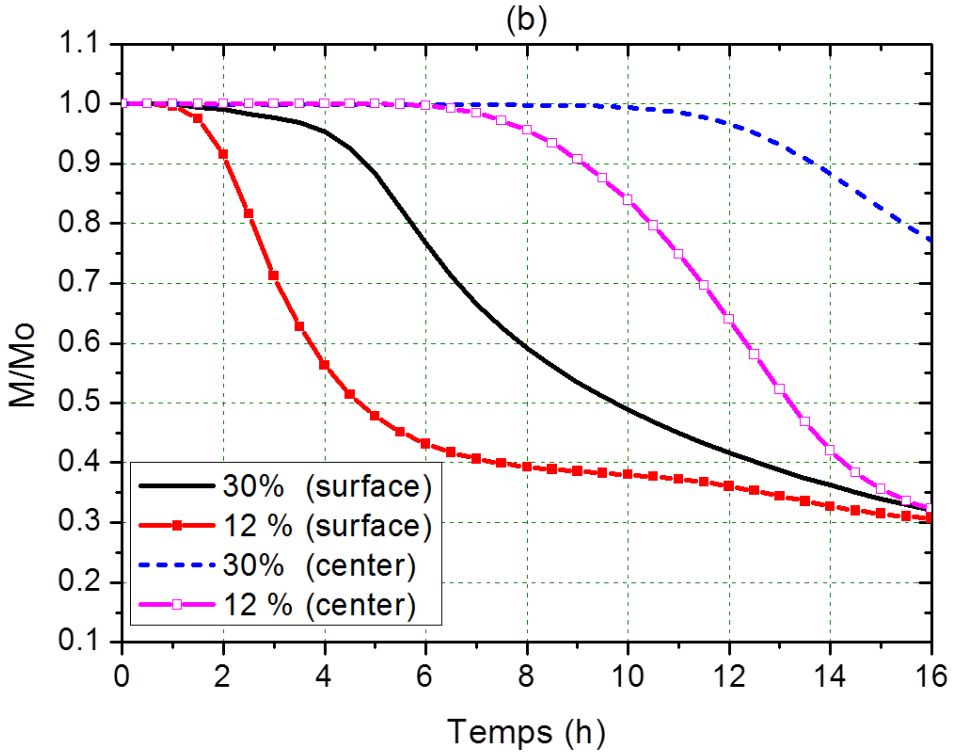

Figure 7. Temperature distribution along the x direction for two moistures conditions (M_0 = 12% and M_0 = 30%, G_m = 0.4).